CHEMISTRY
A EUROPEAN JOURNAL

DOI: 10.1002/chem.200600006

A Positive-Microemulsion Method for Preparing Nearly Uniform Ag_2Se Nanoparticles at Low Temperature

Jian-Ping Ge, Sheng Xu, Li-Ping Liu, and Ya-Dong Li*[a]

Abstract: A positive-microemulsion system (water/sodium linoleate/hexane) was used to make uniform Ag_2Se nanoparticles at low temperature (7–10 °C) within five to ten minutes. The proposed interface-reaction mechanism was corroborated by transmission electron microscopy (TEM), IR spectroscopy, and X-ray photoelectron spectroscopy (XPS) results. This is a general method that is ideal for making other uniform nanoparticles on a large scale through simple precipitation reactions.

Keywords: interfaces · microemulsions · nanostructures · selenium · silver

Introduction

Silver selenide is a special and interesting material, which has been extensively studied in different fields during the past several years. It has two stable solid phases: The low-temperature phase (orthorhombic), β-Ag_2Se, is a narrow-band-gap semiconductor with an energy gap of 0.07 eV at 0 K. The high-temperature phase (body-centered cubic), α-Ag_2Se, is a metallic compound with superionic characteristics; the compound undergoes a reversible first-order phase transition around 407 K with a remarkable change in its electronic property. β-Ag_2Se has proved to be a promising candidate for thermoelectric applications due to its high electrical conductivity, large Seebeck coefficient, and low thermal conductivity.[1] α-Ag_2Se, as a solid electrolyte, is used as an additive in highly conductive composite glasses for batteries, sensors, and displays.[2] Recently, it was reported that a slight alteration of the stoichiometry to Ag_2Se can induce a remarkable magnetoresistance, which is comparable to the giant magnetoresistance perovskites.[3–4]

Because nanoscale materials might have some unique physical properties that rely on the size and morphology of the particles, it would be a great challenge to fabricate Ag_2Se nanostructures of a controllable size. Various methods including organometallic-precursor thermolysis,[5] ultrasonic vibration,[6] photoirradiation,[7] hydrothermal treatment,[8] and template growth[9] have been used to fabricate Ag_2Se orthorhombic nanoparticles. However, it is hard to meet both the criteria that the method be simple and fast, that is, Ag_2Se forms at room temperature in one step, and that the product be composed of dispersive nanocrystals of nearly uniform size.

Here, we reported a low-temperature positive-microemulsion method to prepare uniform-sized Ag_2Se nanoparticles (NPs) by reacting Ag^+ with $SeSO_3^{2-}$. For the first requirement, Na_2SeSO_3[10] is selected as the selenium source because it easily reacts with Ag^+ ions at room temperature without requiring the input of any other forms of energy. Na_2SeSO_3 is much more active than Se powder, and is also less toxic and therefore safer to use than Na_2Se or H_2Se. It is a fast (5–10 min) reaction that would be useful for large-scale production. For the second criterion, a low-temperature positive-microemulsion[11] environment was introduced to protect the products from aggregation and direct them into a relative uniform size. The low temperature (7–10 °C) also helps the formation of nearly uniform Ag_2Se particles by slowing the growth speed and decreasing the surface atom activity. Equations (1) and (2) describe the processes involved:

$$Na_2SO_3 + Se \xrightarrow{\text{reflux}} Na_2SeSO_3 \quad (1)$$

$$Na_2SeSO_3 + 2\,AgNO_3 + H_2O \rightarrow Ag_2Se\downarrow + 2\,NaNO_3 + H_2SO_4 \quad (2)$$

---

[a] J.-P. Ge, S. Xu, L.-P. Liu, Prof. Y.-D. Li
Department of Chemistry
Tsinghua University
Beijing 100084 (P.R. China)
Fax: (+86) 10-6278-8765
E-mail: ydli@mail.tsinghua.edu.cn

Supporting information for this article is available on the WWW under http://www.chemeurj.org/ or from the author.

Results and Discussion

Figure 1 shows the X-ray diffractometry (XRD) pattern of the Ag_2Se NPs. It can be observed from this that orthorhombic Ag_2Se formed in our synthesis. All the characteristic peaks match exactly with the standard JCPDS card (no. 241041). It is reasonable to yield the orthorhombic phase at room temperature because it is a low-temperature stable phase, and all the examples in the literature[6–9] reported the same results. Slight peak broadening indicated that the nanoparticles might have a small size of around 10 nm. From the energy dispersive spectroscopy (EDS) analysis, discussed later, it can be seen that there are very small amounts of sulfur-containing substances in the samples. However, the XRD patterns do not indicate the presence of Ag_2S, Ag_2SO_3, or Ag_2SO_4, which confirms that no crystalline sulfur impurities formed, and therefore the impurity may be neglected in this case.

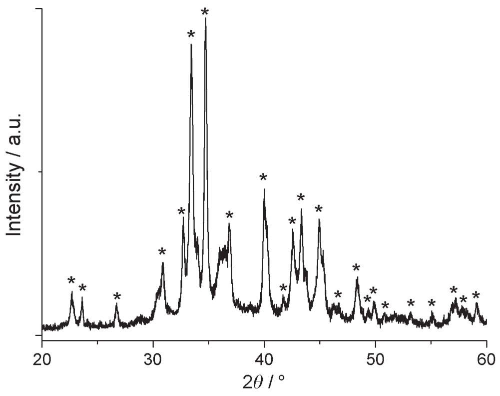

Figure 1. XRD pattern of orthorhombic Ag_2Se nanocrystals. a.u. = arbitrary units.

UV absorption and Raman spectra were also measured to confirm the formation of Ag_2Se. Samples dissolved in *n*-hexane were used for UV measurements. From Figure 2a, the absorption edge was determined at $\lambda = 630$ nm, which is close to the literature value reported for Ag_2Se nanocrystals.[6b,10b] Figure 2b shows the Raman spectrum of the samples. A characteristic peak around $\tilde{\nu} = 143\,cm^{-1}$[12–13] was observed, which is evidence of Ag–Se bond formation.

Transmission electron microscopy (TEM) analysis was used to further explore the crystal structure of the Ag_2Se NPs. Figure 3a,b show the TEM images of sample I (see the Experimental Section) prepared at low temperature. The products are purely uniform particles without any aggregation at all. The size of the particle ranges from 7 to 12 nm, and the average size is calculated to be 10 nm. Figure 3c shows an electron diffraction pattern indicative of many single particles. Figure 3d shows the HRTEM image of a single Ag_2Se NP with a diameter of about 10 nm.

EDS analysis was also used to analyze the dispersive nanocrystals (Figure 3f). Strong Ag and Se peaks undoubtedly confirmed that the product is Ag_2Se. Cu and O peaks come from the carbon-coated copper grid and oxygen in the system, which is a normal observation for TEM samples. The weak Si peak can only be caused by the glass vessels used in the experiments, because no Si-containing reagents were used in this study. The much weaker S peak may come from SO_4^{2-}, which is generated with the release of Se^{2-} from $SeSO_3^{2-}$ [Eq. (2)]. However, according to the XRD results, no obvious Ag_2SO_4 phase forms, which suggests that this rather small sulfur impurity can be ignored in this case. Therefore, the samples are basically pure Ag_2Se nanocrystals.

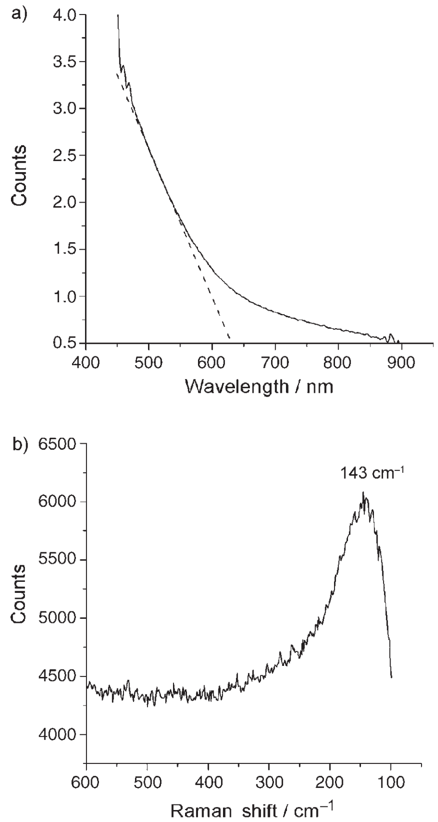

Figure 2. a) UV spectrum of a solution of Ag_2Se in *n*-hexane. b) Raman spectrum of Ag_2Se NPs.

Figure 3g shows the TEM image of sample II (see the Experimental Section) prepared at room temperature. The products were irregular in shape and larger on first sight than sample I. Figure 3e shows the high-resolution transmission electron microscopy (HRTEM) image of a single Ag_2Se nanoparticle with a diameter of about 20 nm. It is a general phenomenon in both samples I and II that some of the NPs have a cavity inside and some do not. Figure 3d,e are representative of two such typical morphologies. Through further HRTEM studies it was found that the peanutlike (Figure 3i) and wormlike (Figure 3h) structures were probably formed by the conjugation of several nearby spherical particles. Lattice faults also appear at the border of two particles.

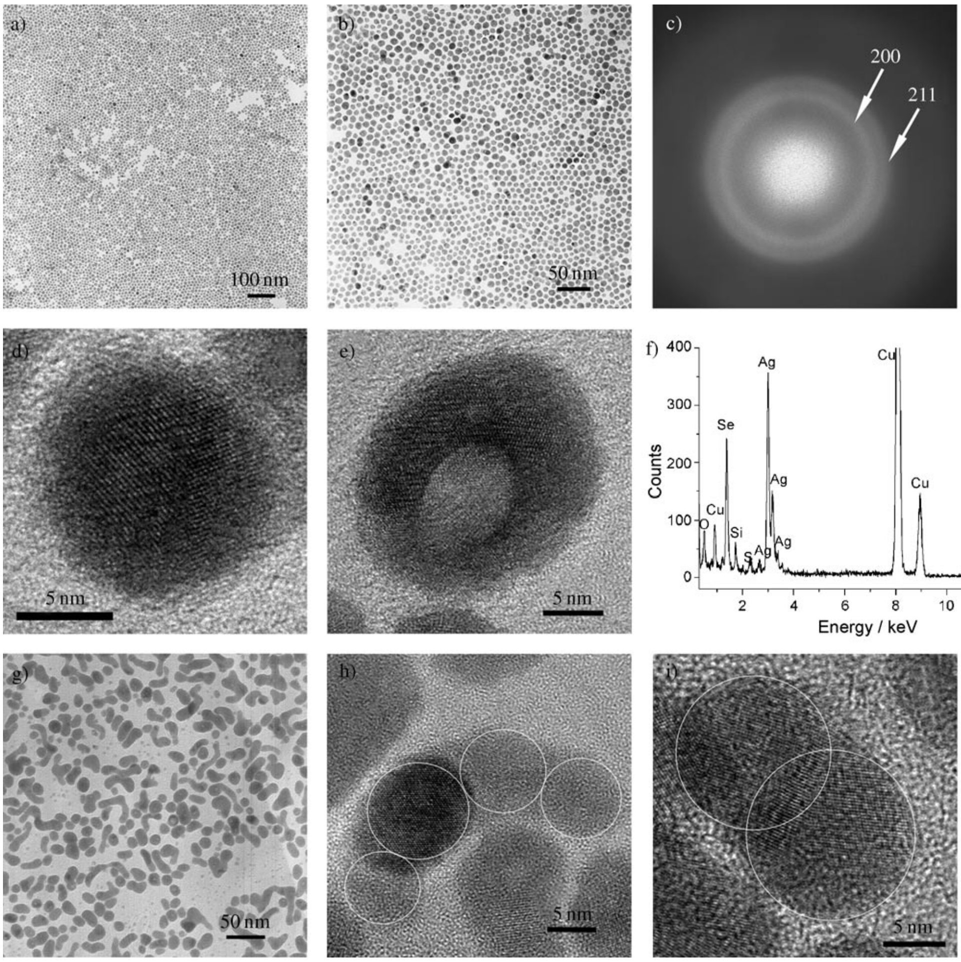

Figure 3. a),b) TEM image, c) electron diffraction and f) EDS analysis of sample I. d),e) HRTEM image of a single particle of sample I and II, respectively. g) TEM and h),i) HRTEM images of sample II.

The TEM results enabled us to answer the question as to why small dispersive Ag_2Se nanoparticles are difficult to obtain. It can be understood from two respects. First, the crystal growth speed of Ag_2Se is very fast even at room temperature due to the large solubility product constant, K_{SP}. Therefore, silver and selenium atoms stack quickly in all space directions without selection, finally resulting in a large irregular crystal, such as sample II. Second, the surface atoms of the small nanoparticles are so active that they may combine with atoms on the surface of another particle, which will also yield irregular crystals. Even in sample I, irregular particles will be generated under exposure to electron-beam irradiation over a long period of time during the TEM analysis. The whole process could be observed clearly and seems to be a strong tendency even with the surfactant protection during the reaction. In our system, a relatively low temperature was used that both slows the growth speed and decreases the surface atom activity, so that uniform-sized Ag_2Se nanoparticles were successfully prepared with this method.

Based on the TEM study and experimental process, a possible positive-microemulsion mechanism (Figure 4) was suggested to explain the formation of 10 nm-sized Ag_2Se NPs. This mechanism includes three steps, which just correspond to the practical manipulation:

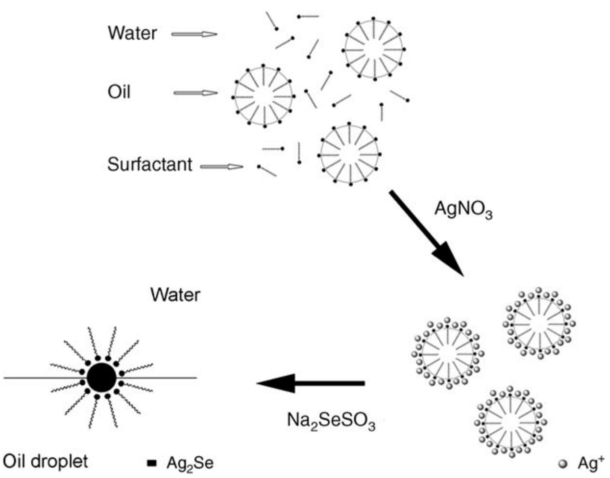

Figure 4. A possible mechanism for the formation of Ag_2Se NPs.

1) In the original solution, all the reagents and solvents added make a positive microemulsion. NaOH reacts with linoleic acid to generate the surfactant, while deionized water and *n*-hexane form the water and oil phase, respectively. Ethanol was added to make the microemulsion more stable. Because the water phase is much larger than the oil phase, the homogeneous solution should be a typical positive microemulsion.
2) When an aqueous $AgNO_3$ solution was added to the solution from step 1, the Ag^+ ions were immobilized on the oil droplet due to the coordination between Ag^+ and $C_{17}H_{31}COO^-$, forming an Ag layer on the outside. This can be confirmed by a simple experiment. At step 2, enough hexane was added to destroy the Ag^+-containing normal microemulsion (see Figure 1a in the Supporting Information), and after several minutes the mixture was separated into an upper nonpolar phase and a lower polar phase with a visible boundary (see Figure 1c in the Supporting Information). If the original speculation of $Ag^+{-}C_{17}H_{31}COO^-$ immobilization to emulsion droplet is true, most of the Ag^+ should be stabilized in the upper phase. We took the same amount of solution from each phase and added the same amount of Na_2SeSO_3 to each. The result showed that most of the Ag^+ was indeed in the upper nonpolar phase.
3) Na_2SeSO_3 was injected into the emulsion and reacted with the Ag^+ ions on the water/oil interface to yield Ag_2Se NPs. The as-made nanoparticles were quickly surrounded with surfactant molecules from both the oil-core surface and the water/ethanol solution. Due to the soft nature of the water/oil interface, a small amount of oil might be embedded in the particles during the fast formation of Ag_2Se. This is a very fast process, and only some of the nanoparticles have a cavity inside.

Further research into the chemical bonding and composition offer some indirect proof to support the above mechanism. The IR spectra (Figure 5) were used to analyze the organic component at the surface. The IR spectrum of Ag_2Se in hexane is similar to that of pure hexane, except for the split peaks from 2800 to 3000 cm^{-1}, which were caused by $C_{17}H_{31}COO^-$ and $C_{17}H_{31}COOH$. The IR spectrum of Ag_2Se NP powder supplies more characteristic peaks. Two strong peaks around $\tilde{\nu}$ = 2920 and 2850 cm^{-1} were attributed to the asymmetric and symmetric stretching vibrations of the C–H bond, respectively. Two strong peaks at $\tilde{\nu}$ = 1560 and 1427 cm^{-1}, which are two characteristic peaks in the IR database for identifying a carboxylic salt, were assigned to the asymmetric and symmetric stretching vibration of the -COO$^-$ group, respectively. A small shoulder around $\tilde{\nu}$ = 1647 cm^{-1} was indexed to the stretching vibration of the C=C double bond. All these peaks provide evidence to support the existence of the $C_{17}H_{31}COO^-$ unit coating the outside of the particle.

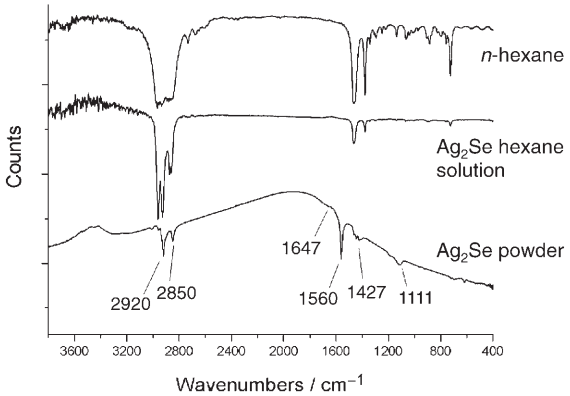

Figure 5. IR spectra of *n*-hexane, a solution of Ag_2Se in hexane, and Ag_2Se NPs (powder).

X-ray photoelectron spectroscopy (XPS; Figure 6) was used to analyze the inorganic component and chemical bonding at the surface. First, the XPS survey spectrum only shows the peaks of Ag, Se, O, and C, illustrating the high purity of the sample. The binding energies of Se 3d and Ag 3d$_{5/2}$ are 53.85 and 367.85 eV (standard: Ag_2Se 367.8 eV), respectively, which is undoubtedly in accordance with the

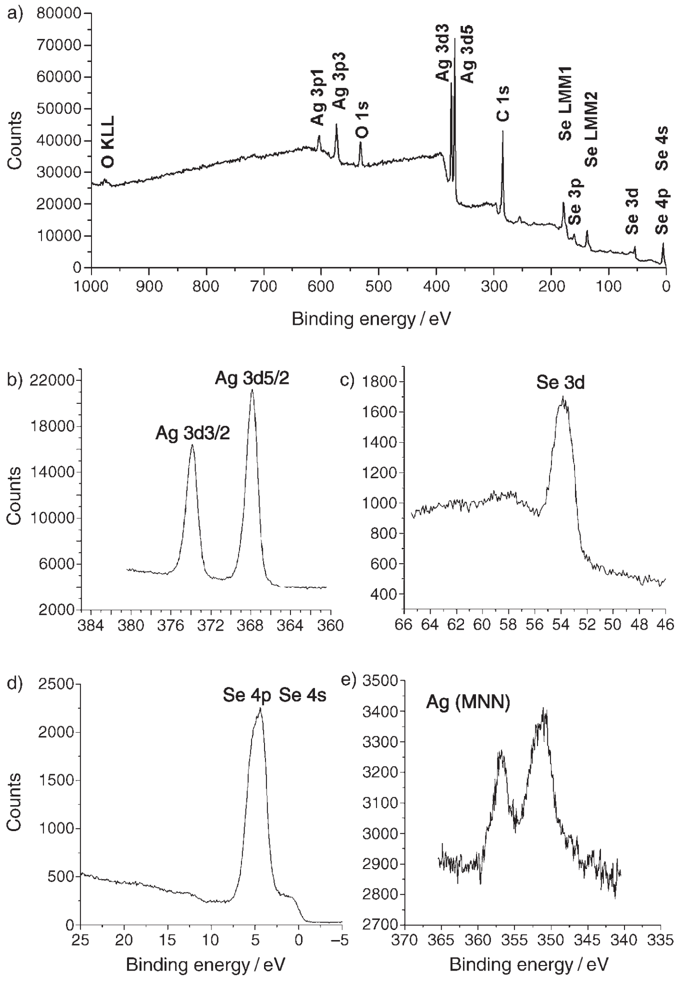

Figure 6. XPS spectra of Ag_2Se NPs: a) survey spectrum; b) Ag 3d spectrum; c) Se 3d spectrum; d) valance band spectrum of Se; e) Auger spectrum of Ag.

standard data. The valance band spectrum (Figure 6d) shows a peak at about 5 eV, which might be the signal of Se 4s and Se 4p. Quantification of the XPS survey spectrum peaks gives the ratio of Ag to Se as 2.52:1. The excess of surface silver implies that it might bond with another atom besides Se. Therefore, an Auger electron spectrum (Figure 6e) was carried out to give more definite information about the probable chemical environment of silver. Two peaks at 351.15 and 356.81 eV were found to be close to values of Ag_2Se (351.4 eV) and Ag_2O (356.6 eV), respectively, from the handbook. It suggests that the excess Ag should bond with the O atom of $C_{17}H_{31}COO^-$, which also offers indirect proof of the mechanism.

Furthermore, to examine the correctness of the proposed mechanism we designed two Ag-related experiments, in which Ag NPs and Ag_2S NPs could also be prepared in this positive-microemulsion system (see Figures 2 and 3 in the Supporting Information). First, an identical positive microemulsion was made at room temperature. Second, Ag^+ ions were immobilized on the oil droplets. Third, $N_2H_4{\cdot}H_2O$ and Na_2S solution were injected into the emulsion to yield Ag and Ag_2S nanoparticles, respectively. These two examples strongly support the mechanism proposed, and also reveal its universality.

Conclusion

In conclusion, a low-temperature, fast synthesis of nearly uniform orthorhombic Ag_2Se nanoparticles was developed in this study. A possible positive-microemulsion mechanism was suggested, and TEM, IR, and XPS results support this mechanism from various aspects. The method developed in this paper to form uniform nanoparticles has several advantages over former reports:[14] 1) The synthesis is accomplished at room temperature. If high crystallinity is not required, this method is also suitable for many other materials, such as sulfides, fluorides, and phosphates. 2) It is a fairly fast method to make particles, and the size of the particle may be determined by the original microemulsion, not by the length of the reaction time. 3) Because the system is a positive microemulsion and the solubility of the inorganic reagents is good, it is an ideal and general method for making other uniform nanoparticles on a large scale through simple precipitation reactions.

Experimental Section

Materials: All the reagents used in this work, including NaOH, linoleic acid (LA, $C_{17}H_{31}COOH$), C_2H_5OH, *n*-hexane, $AgNO_3$, Na_2SO_3, Se powder, $N_2H_4{\cdot}H_2O$, and Na_2S, were A.R. reagents from the Beijing Chemical Factory, China. The Na_2SeSO_3 solution (selenium source) was prepared by refluxing selenium powder (5 mmol) and Na_2SO_3 (5 mmol) in distilled water (50 mL) for 1 h.

Synthesis: In a typical process to prepare sample I, first, NaOH (100 mg) and LA (1.9 mL) were dissolved in the mixture of deionized water (15 mL), C_2H_5OH (15 mL), and *n*-hexane (1 mL) to form a transparent microemulsion. Second, $AgNO_3$ (1 mmol) dissolved in deionized water (5 mL) was added to the solution under vigorous stirring, forming a white Ag^+-containing emulsion quickly. Third, after the emulsion had been maintained at 7–10 °C in the water bath, Na_2SeSO_3 solution (5 mL) was injected into it. The solution changed from transparent to black in three seconds, and was kept stirring for 5–10 min. After the reaction, *n*-hexane (20 mL) was added to destroy the microemulsion and extract the LA-coated Ag_2Se NPs into the oil phase (Figure 1b in the Supporting Information), which was centrifuged to give Ag_2Se NPs by adding C_2H_5OH. Then, the samples were washed several times by dissolving in hexane coupled with precipitating from ethanol to remove LA residues on the particle surface. Finally, these NPs were dissolved in hexane for storage. For sample II, a similar process was used except that NaOH (200 mg) and LA (3.8 mL) were added and the reaction was carried out at room temperature (25–30 °C).

For XRD, Raman, IR, and XPS analyses, Ag_2Se NPs were directly precipitated from a high-concentration solution of Ag_2Se in hexane by adding an adequate amount of ethanol. After drying at 50 °C for 4 h, the gel was ground into a powder for the measurement.

Characterization: The samples were characterized by using a Rigaku D/max 2550 X-ray diffractometer. The size and morphology of the nanoparticles were obtained by using a JEOL JEM-1200EX transmission electron microscope and a Tacnai TF20 high-resolution transmission electron microscope. Energy dispersive spectroscopy (EDS) was also recorded by using the latter. The electronic absorption spectra were obtained on a Hitachi U-3010 UV-visible spectrometer. The IR spectra were recorded on a Nicolet 560 FTIR spectrophotometer. Raman spectra were recorded with an RM 2000 microscopic confocal Raman spectrometer (Renishaw PLC, England) employing a $\lambda = 514$ nm laser beam. X-ray photoelectron spectroscopy (XPS) was carried out using a PHI Quantera SXM.

Acknowledgements

This work was supported by the National Science Foundation of China (NSFC) (90406003) and the State Key Project of Fundamental Research for Nanomaterials and Nanostructures (2003CB716901).

---

[1] M. Ferhat, J. Nagao, *J. Appl. Phys.* **2000**, *88*, 813.

[2] a) P. Boolchand, W. J. Bresser, *Nature* **2001**, *410*, 1070; b) Y. Utsugi, *Phys. Rev. B* **1997**, *55*, 10800.

[3] a) R. Xu, A. Husmann, T. F. Rosenbaum, M. L. Saboungi, J. E. Enderby, P. B. Littlewood, *Nature* **1997**, *390*, 57; b) M. M. Parish, P. B. Littlewood, *Nature* **2003**, *426*, 162; c) A. A. Abrikosov, *Phys. Rev. B* **1998**, *58*, 2788.

[4] a) M. Lee, T. F. Rosenbaum, M. L. Saboungi, H. S. Schnyders, *Phys. Rev. Lett.* **2002**, *88*, 066602; b) M. Kreutzbruck, B. Mogwitz, F. Gruhl, L. Kienle, C. Korte, J. Janek, *Appl. Phys. Lett.* **2005**, *86*, 072102; c) A. Husmann, J. B. Betts, G. S. Boebinger, A. Migliori, T. F. Rosenbaum, M. L. Saboungi, *Nature* **2002**, *417*, 421.

[5] M. T. Ng, C. Boothroyd, J. J. Vittal, *Chem. Commun.* **2005**, 3820.

[6] a) R. Harpeness, O. Palchik, A. Gedanken, V. Palchik, S. Amiel, M. A. Slifkin, A. M. Weiss, *Chem. Mater.* **2002**, *14*, 2094; b) J. Xiao, Y. Xie, R. Tang, W. Luo, *J. Mater. Chem.* **2002**, *12*, 1148.

[7] a) Z. Y. Jiang, R. B. Huang, S. Y. Xie, Z. X. Xie, L. S. Zheng, *J. Solid State Chem.* **2001**, *160*, 430; b) Y. L. Yan, X. F. Qian, H. J. Xu, J. Yin, Z. K. Zhu, *Inorg. Chem. Commun.* **2003**, *6*, 34.

[8] a) Y. Jiang, B. Xie, J. Wu, S. Yuan, Y. Wu, H. Huang, Y. Qian, *J. Solid State Chem.* **2002**, *167*, 28; b) S. K. Batabyal, C. Basu, A. R. Das, G. S. Sanyal, *Cryst. Growth Des.* **2004**, *4*, 509.

[9] a) B. Gates, Y. Wu, Y. Yin, P. Yang, Y. Xia, *J. Am. Chem. Soc.* **2001**, *123*, 11500; b) U. Jeong, Y. Xia, *Angew. Chem.* **2005**, *117*, 3159; *Angew. Chem. Int. Ed.* **2005**, *44*, 3099.

[10] a) X. D. Ma, X. F. Qian, J. Yin, Z. K. Zhu, *J. Mater. Chem.* **2002**, *12*, 663; b) B. Pejova, M. Najdoski, I. Grozdanov, S. K. Dey, *Mater. Lett.* **2000**, *43*, 269.

[11] a) M. Li, H. Schnablegger, S. Mann, *Nature* **1999**, *402*, 393; b) F. T. Quinlan, J. Kuther, W. Tremel, *Langmuir* **2000**, *16*, 4049; c) D. Ingert, M. P. Pileni, *Adv. Funct. Mater.* **2001**, *11*, 136.

[12] M. N. Kozicki, M. Mitkova, J. Zhu, M. Park, *Microelectron. Eng.* **2002**, *63*, 155.

[13] K. Ogusu, T. Kumagai, Y. Fujimori, M. Kitao, *J. Non-Cryst. Solids* **2003**, *324*, 118.

[14] a) C. B. Murray, D. J. Norris, M. G. Bawendi, *J. Am. Chem. Soc.* **1993**, *115*, 8706; b) X. Peng, L. Manna, W. Yang, J. Wickham, E. Scher, A. Kadavanich, A. P. Alivisatos, *Nature* **2000**, *404*, 59; c) J. Joo, H. B. Na, T. Yu, J. H. Yu, Y. W. Kim, F. Wu, J. Z. Zhang, T. Hyeon, *J. Am. Chem. Soc.* **2003**, *125*, 11100; d) S. Sun, H. Zeng, D. B. Robinson, S. Raoux, P. M. Rice, S. X. Wang, G. Li, *J. Am. Chem. Soc.* **2004**, *126*, 273; e) X. Wang, J. Zhuang, Q. Peng, Y. Li, *Nature* **2005**, *437*, 121.

Received: January 4, 2006